MSIV LEAKAGE IODINE TRANSPORT ANALYSIS

Prepared for:
U.S. Nuclear Regulatory Commission
under
Contract NRC-03-87-029, Task Order 75

Prepared by:
J.E. Cline & Associates, Inc.

March 26, 1991

TABLE OF CONTENTS

LIST OF TABLES

LIST OF FIGURES

MSIV LEAKAGE IODINE TRANSPORT ANALYSIS

1.0 INTRODUCTION AND SUMMARY

1.1 GASEOUS IODINE TRANSPORT

Gaseous iodine and airborne particulate material deposit on surfaces. Basic chemical and physical principals predict this behavior and several laboratory and in–plant studies[1-13] have supported and demonstrated this deposition wherein gaseous iodine deposits by chemical adsorption and particulates deposit through a combination of sedimentation, molecular (Brownian) diffusion, turbulent (momentum) diffusion, and impaction. Gaseous iodine exists in nuclear power plants in several forms that are commonly described[5,6,10-12] as three forms, elemental (I_2), hypoiodous acid (HOI) and organic (CH_3). Each of these forms deposits on surfaces at a different rate, described by a parameter known as a deposition velocity. The I_2 form, being the most reactive, has the largest deposition rate, and organic iodide has the smallest (by more than a factor of 100). Further, studies of in–plant airborne iodine show[10-12] that iodine deposited on the surfaces undergoes both physical and chemical changes and can either be re-emitted as an airborne gas (resuspension) or become permanently fixed to the surface (fixation). The data also show that in the resuspension process, the iodine can change its form (conversion) so that iodine deposited as one form (usually elemental) can reappear as itself or as another (HOI or organic) iodine form. Conversion can be described in terms of resuspension rates that are different for each iodine species. Chemical surface fixation can similarly be described in terms of a surface fixation rate constant. Iodine absorbed on particulate matter and deposited on surfaces can also resuspend[11-12] as gaseous iodine. The in-plant studies also suggested that this iodine attached to particulates could be treated as "elemental iodine" (this would not apply to CsI particles). For the low–velocity transport in the present study, particulates would deposit quantitatively with near 100% efficiency. This analysis, therefore, treats airborne particulate iodine as though it were gaseous elemental iodine.

Deposition, resuspension, conversion and surface fixation of gaseous iodine have effects upon the transport of iodine in any air-stream pathway. Effects include:

1. a reduction in the concentration of airborne activities along the pathway (losses),

2. a shifting in the iodine molecular form distribution from elemental toward the less reactive organic iodide (conversion),

3. a greater relative loss of the shorter–lived iodine isotopes than of the longer lived [129]I, ^{131}I and [133]I (aging).

For transport of airborne iodine in air streams through pipes, these phenomena can result in losses of elemental iodine and conversion of a portion of the deposited iodine to airborne organic iodine. Gaseous iodine losses are very dependent upon residence time,

1

i.e. path length and sample velocities within the lines, and on temperature. Deposition and resuspension result in transmissions that exhibit a transient behavior, rising to an equilibrium value for gaseous iodine that often requires long times (hours or days) to reach. The transient behavior is important under accident conditions where an abrupt rise in emissions may occur.

1.2   IODINE TRANSPORT MODEL

1.2.1   TRANSPORT THROUGH PIPES

The transport of gaseous iodine has been studied for many years and several groups have proposed[3,9-12] models to describe the observed phenomena. The simplest model that treated both deposition and resuspension[11] described deposition of reactive species on surfaces, species transformations on the surfaces, and resuspension of the deposited radioiodine. These phenomena are chemically complicated and not well understood, and the descriptions were in terms of rate constants, experimentally measured. The original model assumed that the total air volume and the interior surface of the line could each be treated as a single compartment and that all deposited iodine remained available for resuspension except for that lost through radioactive decay. An additional assumption was that the air stream transit time through the pathway was short compared to the times considered and that the air stream was instantaneously mixed within the entire volume. The assumption of a single compartment is not valid for long lines and was soon modified[3] to divide a path along multiple sections of line for computation. The current model views a path as a sequence of small segments that use the assumption of instantaneous and homogeneous mixing, and applies the computation to each segment, passing the results as input to the next segment. The number of segments depends upon the parameters of the line and flow rate and can be as many as 100,000 for a long, large–diameter pipe and a low flow. Resuspension data taken after the source of injected iodine was removed showed a monotonic decrease in resuspension rates[3] with time. An alternate explanation is that chemical reactions occurred on the surface that permanently fixed a portion of the iodine to the surface, a phenomenon consistent with known behavior of reactive iodine. Consequently, the model was modified to include a chemical bonding reaction rate to iodine deposited on the surface. Figure 1 shows a diagram of the compartments of the present model. Each line segment has five compartments that are the concentrations of the three airborne iodine species, the surface that contains iodine available for resuspension, and surface iodine that has reacted and is fixed on the surface. All iodine in the segment undergoes radioactive decay. The resulting concentration from each segment of length serves as the input to the next segment. To observe the time dependence of the transport, the time of the calculation period is broken into small time divisions where the assumptions of instantaneous equilibrium is more valid. A typical computation breaks the time of the study into 100 divisions, each of which should be less than 5% of the decay half life and much larger than the transit time through the length segment.
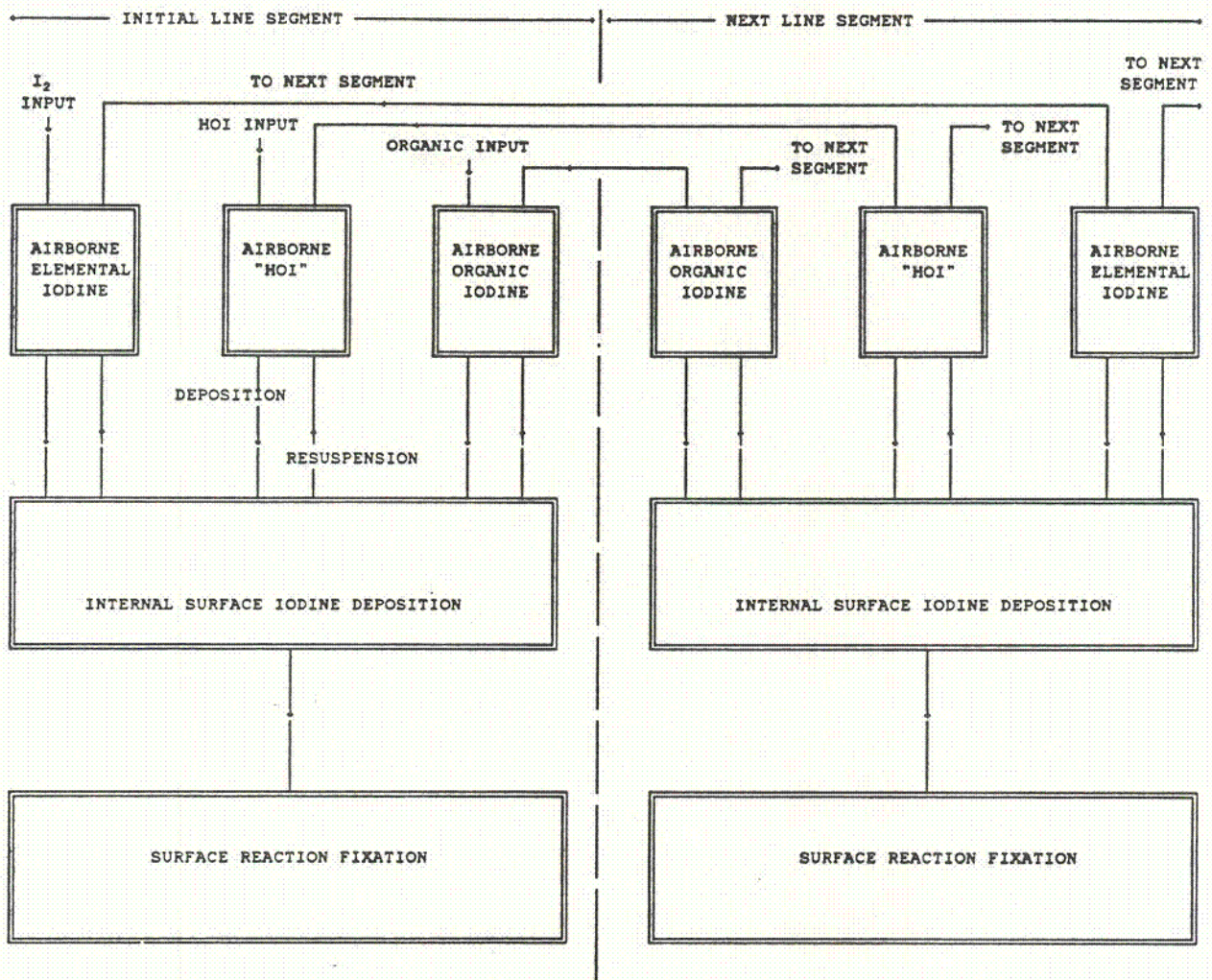
FIGURE 1. Schematic diagram indicating the flow path for the transport of airborne gaseous iodine along the length of a component. The sketch shows the five compartments of each of the first two volume segments into which the line was divided: the path through the remainder is similar to that shown.

The model initially developed by SAIC describes deposition, resuspension and conversion of iodine in terms of rate coefficients in four differential equations describing, respectively, airborne elemental, HOI and organic, and surface activities. These equations are:

$$\frac{dI}{dt} - (Q_S \times C_S \times P_I) - (\mu_I + \frac{Q}{V} + \lambda) \times I + \nu_I \times S,$$

$$\frac{dH}{dt} - (Q_S \times C_S \times P_H) - (\mu_H + \frac{Q}{V} + \lambda) \times H + \nu_H \times S,$$

$$\frac{dO}{dt} - (Q_S \times C_S \times P_O) - (\mu_O + \frac{Q}{V} + \lambda) \times O + \nu_O \times S,$$

and

$$\frac{dS}{dt} - \mu_I \times I + \mu_H \times H + \mu_O \times O - (\nu_I + \nu_H + \nu_O + \phi) \times S,$$

where:

Q_S is the stream flow rate (cc/sec),
P_I is the partitioning fraction of iodine in the stream as I_2,
P_H is the partitioning fraction of iodine in the stream as HOI,
P_O is the partitioning fraction of iodine in the stream as organic iodine,
C_S is the inlet iodine concentration in the stream (activity/cc),
μ_I is the deposition rate for elemental iodine onto the surfaces
        (= $d_I \times S/V$, d_I=deposition velocity, V=volume, S=surface area) (sec$^{-1)}$,
μ_H is the deposition rate for HOI onto the surfaces
        (= $d_H \times S/V$, d_H=deposition velocity, V=volume, S=surface area) (sec$^{-1)}$,
μ_O is the deposition rate for organic iodine onto the surfaces
        (= $d_O \times S/V$, d_O=deposition velocity, V=volume, S=surface area) (sec$^{-1)}$,
I is the total airborne elemental iodine (activity in length segment),
H is the total airborne HOI (activity in length segment),
O is the total airborne organic iodine (activity in length segment),
S is the total surface iodine (activity on segment surface),
ν_I is the resuspension rate of elemental iodine from the surface
        (fractional resuspension/sec),
ν_H is the resuspension rate of HOI from the surface
        (fractional resuspension/sec),
ν_O is the resuspension rate of organic iodine from the surface
        (fractional resuspension/sec), and
ϕ is the surface reaction fixation rate (fractional fixation/sec).

Values of the parameters are model dependent, extracted from experimental measurements of transmission or concentration loss rates. However, except for

measurements with transmission factors of less than about 50%, values of deposition velocities are nearly independent of the model. The equations apply to each length segment of a line.

1.2.2 TRANSPORT THROUGH CONDENSER

Computations of iodine transport through the condenser treat the flow as a dilution flow rather than the plug flow as in the pipes. The assumption is that the input iodine mixes instantaneously, within the time segment, with a volume of air in the condenser and the diluted air exhausts at the same rate as the input rate. Additional assumptions in deriving the first set of equations are that there is no surface deposition of low-reactive species, HOI and organic iodine. This model does not consider the elemental iodine input to the condenser that is described separately. For non-reactive iodine, the equation expressing the concentration of each species of iodine in the condenser air volume as a function of time is:

$$C_{cond}(t) - \frac{Q}{V} e^{-kt} (\int_0^t C(t) e^{kt} dt - C(0))$$

where:

- Q is the inlet and outlet leak rate,
- $C(t)$ is the inlet iodine concentration of that species at time, t,
- k is the sum of Q/V and λ, the decay constant, and
- $C_{cond}(t)$ is the airborne concentration in the condenser.

For numerical integration, the equation becomes:

$$C_{cond}(t-t_n) - (\frac{Q}{V}) e^{-kt_n} \sum_{i-1}^{n} [C(t) e^{kt_i} \Delta t_i - C(0)]$$

The condenser model treats elemental iodine separately. Any elemental iodine remaining in the inlet stream, because of the large volume and very low flow rate, will deposit on the internal surfaces of the condenser where resuspension of other species will occur. Any resuspended elemental iodine will redeposit whereas resuspended HOI and organic iodine add to their respective concentrations in the air volume. Under these conditions, the equation for the total iodine deposited on the condenser surfaces as a function of time is:

$$S_{cond}(t-t_n) - Qe^{-k_1 t_n} \sum_{i=1}^{n} [C_{E-i}(t) e^{k_1 t_i} \Delta t_i - S(0)]$$

where:

      k_1 is the sum of the HOI and organic resuspension and the surface fixation rates,

      C_{E-i} is the inlet elemental concentration at time t_i,

      $S(0)$ is the surface activity at time 0, and

      $S_{cond}(t)$ is the surface activity in the condenser.

The concentrations of HOI and organic iodine resuspended from iodine on the condenser surfaces is given in terms of the total surface activity as:

$$H_{cond}(t-t_n) - (\frac{v_H}{V}) e^{-\frac{Q}{V} t_n} \sum_{i=1}^{n} [S_i(t) e^{\frac{Q}{V} t_i} \Delta t_i - H(0)]$$

and

$$O_{cond}(t-t_n) - (\frac{v_O}{V}) e^{-\frac{Q}{V} t_n} \sum_{i=1}^{n} [S_i(t) e^{\frac{Q}{V} t_i} \Delta t_i - O(0)]$$

where:

      Q is the inlet and outlet leak rate,

      V is the volume of mixing air in the condenser,

      v_H is the resuspension rate for HOI,

      v_O is the resuspension rate for organic iodine,

      S_i is the surface activity at time, t_i,

      $H(0)$ and $O(0)$ are the activities at t=0,

      $H_{cond}(t)$ is the airborne HOI concentration in the condenser, and

      $O_{cond}(t)$ is the airborne organic concentration in the condenser.

These concentrations are added to the concentrations resulting from these species entering the condenser to obtain the total concentration of each specie.

2.0   EVALUATION AND SELECTION OF DEPOSITION, RESUSPENSION AND FIXATION CONSTANTS FOR TRANSPORT MODEL

     2.1 DATA BASE

Several laboratories[1-9] have reported measurements of the deposition velocities and SAIC[3,8] has reported a few measurements of resuspension and fixation rates in measurements using simulated sampling lines. The models use these parameters to predict transmission factors for gaseous iodine in sample lines, for both equilibrium and

6

transient behavior. Table 1 presents a summary of published and unpublished data found in literature searches. The table cites the reference for the data. The data for the fixation rate and much of the data for the elemental iodine resuspension rate is from unpublished results of laboratory tests on simulated utility plant sampling lines of varying lengths, diameters and flow rates. In this batch, only the data from BWR "D" allowed estimates of resuspension rates for HOI and organic components. The evaluation assumed an average value of resuspension for the elemental component. Using an average value for the fixation constant from the utility data and the current SAIC model, described above also permitted re-analysis of the data in reference 3. Table 2 shows the results of this re-analysis and Table 1 incorporates these analysis results. Deposition velocities for HOI and organic iodine, shown in Table 2, are values used in the analyses. Their values were estimated from in-plant iodine species data in references 10-12. Deposition velocities are sufficiently low that the deposition of these two iodine forms is not significant in most applications of the models. The other data in Table 1 are from all sources identified in the extensive library literature search. The search yielded no data for resuspension or fixation rates at temperatures other than ambient. The last entries in the table are from analyses of data collected[10,11] from 1971 to 1978 in operating BWR plants. The data are from steam-jet-air-ejector delay lines, gland-seal exhausts, condenser-bay steam leaks, and ventilation air exhaust streams. The analysis of these data for deposition and resuspension rates have considerable uncertainties because of multiple inputs to each plant stream.

The bottom of Table 1 shows averages and standard deviations of all the measurements of deposition velocities, and resuspension and fixation rates at ambient temperature (25-35°C). (The averaging included neither the data of Kabat which have deposition velocities that appear anomalously low nor the TMI-2 data that are for organic deposition and resuspension on specially painted surfaces.) The large standard deviations reflect both the difficulties in the measurements and the validity of the assumptions in the model that extract the coefficients from the data. The parameters have uncertainties of 40-75%.

Figure 2 shows a plot of the measured elemental iodine deposition velocities, given in Table 1, as a function of temperature. The plot is of the logarithm of the deposition velocity against the reciprocal of the absolute temperature (a typical presentation of chemical reaction rate). The Figure demonstrates the considerable scatter in the data. Figure 2 also shows a least-squares fit to the data in Table 1.

2.2   COEFFICIENT EVALUATION AND SELECTION

Data in Tables 1 and 2, being the only data identified, must serve as the bases for estimating the deposition velocities, resuspension rates and surface fixation rates as a function of temperature over the range of temperatures expected in the MSIV leakage dose-consequence evaluation. The following represents best estimates of the temperature coefficients as applied to the SAIC or similar iodine transport models.

REFERENCE	MATERIAL	TEMPERATURE (oC)	DEPOSITION VELOCITY (cm/s)	RESUSPENSION RATE (1/sec) ELEMENTAL	HOI	ORGANIC	FIXATION RATE (1/s)
1 NICOLOSI et.al.	SS-304	300	2.0E-06				
	SS-304	300	1.0E-05				
	SS-304	600	8.0E-05				
	SS-304	900	5.0E-05				
	SS-304	1130	9.0E-04				
2 GENCO et.al.	SS-304	100	7.0E-01				
	SS-304	125	3.0E-02				
	SS-304	125	2.0E-02				
	SS-304	125	8.0E-03				
	SS-304	125	5.0E-03				
	SS-304	225	1.0E-03				
	SS-304	225	2.0E-04				
	SS-304	325	7.0E-05				
	SS-304	325	8.0E-06				
	SS-304	625	2.0E-05				
3 UNREIN et. al.	SS-304	30	2.0E-02	6.0E-06	4.1E-08	6.9E-08	
	SS-304	30	3.6E-02	5.0E-06	4.1E-08	6.9E-08	
	SS-304	30	5.3E-02	7.0E-06	4.1E-08	6.9E-08	
	SS-304	30	2.0E-02	1.0E-05	1.1E-07	1.1E-07	
	SS-304	30	2.2E-02	1.0E-06	6.9E-08	6.9E-08	
	SS-304	30	1.8E-02	1.0E-06	6.9E-08	4.1E-08	
	SS-304	30	1.2E-02	7.0E-06	1.1E-07	1.1E-07	
	SS-304	30	1.0E-02	1.0E-05	1.1E-07	1.1E-07	
4 NEBEKER et. al. *	SS-304	80	6.5E-02				
5 MANDLER et. al. Methyl iodine injections	CONTAINMENT COUPONS	30	1.5E-03	1.0E-05			
			7.5E-04				
			1.5E-03				
			1.6E-03				
6 CLINE et.al.	PAINTED SS	30	7.0E-05			5.0E-10	
7 LORENZ et. al.	SS-304	150-550	log(v)= 2.14x1000/T-7.8	1.2E-05			
8 BWR "A"	SS-304	30	0.027	4.1E-06			2.9E-06

TABLE 1. SUMMARY OF EXPERIMENTALLY MEASURED DEPOSITION, RESUSPENSION AND FIXATION RATE CONSTANTS.

8

		N					
(SAIC REPORT, OCT 88)		30	0.003	5.7E-07			1.3E-06
PWR "A"		30	0.041	1.8E-06			2.1E-06
(SAIC REPORT, DEC 88)		30	0.038	2.4E-06			2.4E-06
		30	0.024	1.4E-07			2.2E-06
		30	0.041	1.8E-06			2.1E-06
		30	0.038	2.4E-06			2.4E-06
		30	0.020	1.4E-07			2.2E-06
		30	0.036	3.6E-06			1.8E-06
		30	0.021	7.0E-07			6.0E-06
BWR "B"		30	0.012	8.0E-07			5.6E-06
(SAIC-89/1422,JUN 90)		30	0.039	1.1E-06			3.8E-06
		30	0.039	1.1E-06			3.8E-06
		30	0.043	8.5E-06			1.1E-07
		30	0.090	3.6E-06			2.9E-06
		30	0.040	1.3E-06			5.6E-07
		30	0.018	4.0E-06			5.0E-07
		30	0.039	3.1E-06			3.3E-06
PWR "B"		30	0.018	2.2E-06			4.3E-06
(SAIC REPORT, JUL 89)							
BWR "C"		30	0.040	3.5E-06			2.8E-06
(SAIC REPORT, SEP 89)		30	0.005	6.4E-06			5.0E-07
PWR "C"		30	0.020	9.7E-07			1.3E-06
(SAIC-89/1756,DEC 89)							
PWR "D"		30	0.042	3.0E-06			3.4E-06
(SAIC-90/1355,AUG 90)		30	0.026	5.2E-07			2.1E-06
		30	0.063	4.2E-07			5.1E-06
		30	0.040	1.1E-06			1.4E-06
		30	0.051	6.0E-06			6.0E-07
BWR "D"		30	0.026	2.2E-06	1.1E-07	2.0E-07	
(SAIC-LETTER, OCT 90)							
9	SS-304	23	0.0016				
KABAT	CARBON ST.	23	0.0013				
10-12		35	0.045	2.2E-06	1.1E-07	6.1E-07	
(AEC IN-PLANT MEAS.)							
PELLETIER et.al.							
* AVERAGE OF SEVERAL	AVERAGE:	0.026	3.2E-06	7.8E-08	9.4E-08	2.6E-06
MEASUREMENTS ON COUPONS	STD:	0.020	2.7E-06	3.0E-08	4.4E-08	1.5E-06

6

TABLE 1. (continued) SUMMARY OF EXPERIMENTALLY MEASURED DEPOSITION, RESUSPENSION AND FIXATION RATE CONSTAN

						REANALYSIS OF THE DATA IN REFERENCE 3							
				TRANS-	RESUSPENSION (%)			DEPOSITION VELOCITY (cm/sec)			RESUSPENSION RATE (1/sec)		
DIAMETER (cm)	LENGTH (cm)	FLOW RATE (cc/sec)	INJECTION TIME(sec)	MISSION (%)	I–2	HOI	ORGANIC	I–2	HOI	ORGANIC	I–2	HOI	ORGANIC
2.22	3048	1416	4320	75	96.6	1.0	2.4	0.020	0.0022	4.4E–05	2.3E–06	4.1E–08	6.9E–08
2.22	1524	1416	4320	78	96.2	1.3	2.6	0.036	0.0022	4.4E–05	2.3E–06	4.1E–08	6.9E–08
1.91	4293	944	1800	23	88.5	7.0	4.5	0.095	0.0022	4.4E–05	2.3E–06	4.1E–08	6.9E–08
1.91	4293	944	7560	62	88.0	8.0	4.0	0.020	0.0022	4.4E–05	2.3E–06	1.1E–07	1.1E–07
0.64	4267	28.3	1800	0.13	65.0	23.0	12.0	0.022	0.0022	4.4E–05	2.3E–06	6.9E–08	6.9E–08
0.64	4267	28.3	7560	0.50	38.0	36.0	25.0	0.018	0.0022	4.4E–05	2.3E–06	6.9E–08	4.1E–08
2.21	7803	944	15480	58	90.7	5.6	3.7	0.012	0.0022	4.4E–05	2.3E–06	1.1E–07	1.1E–07
2.12	1321	1321	15480	72	90.8	5.5	3.8	0.010	0.0022	4.4E–05	2.3E–06	1.1E–07	1.1E–07

TABLE 2. SUMMARY OF RE-ANALYSIS RESULTS FOR THE DATA OF UNREIN (REFERENCE 3).

10

DISTRIBUTION OF MEASURED DEPOSITION VELOCITIES
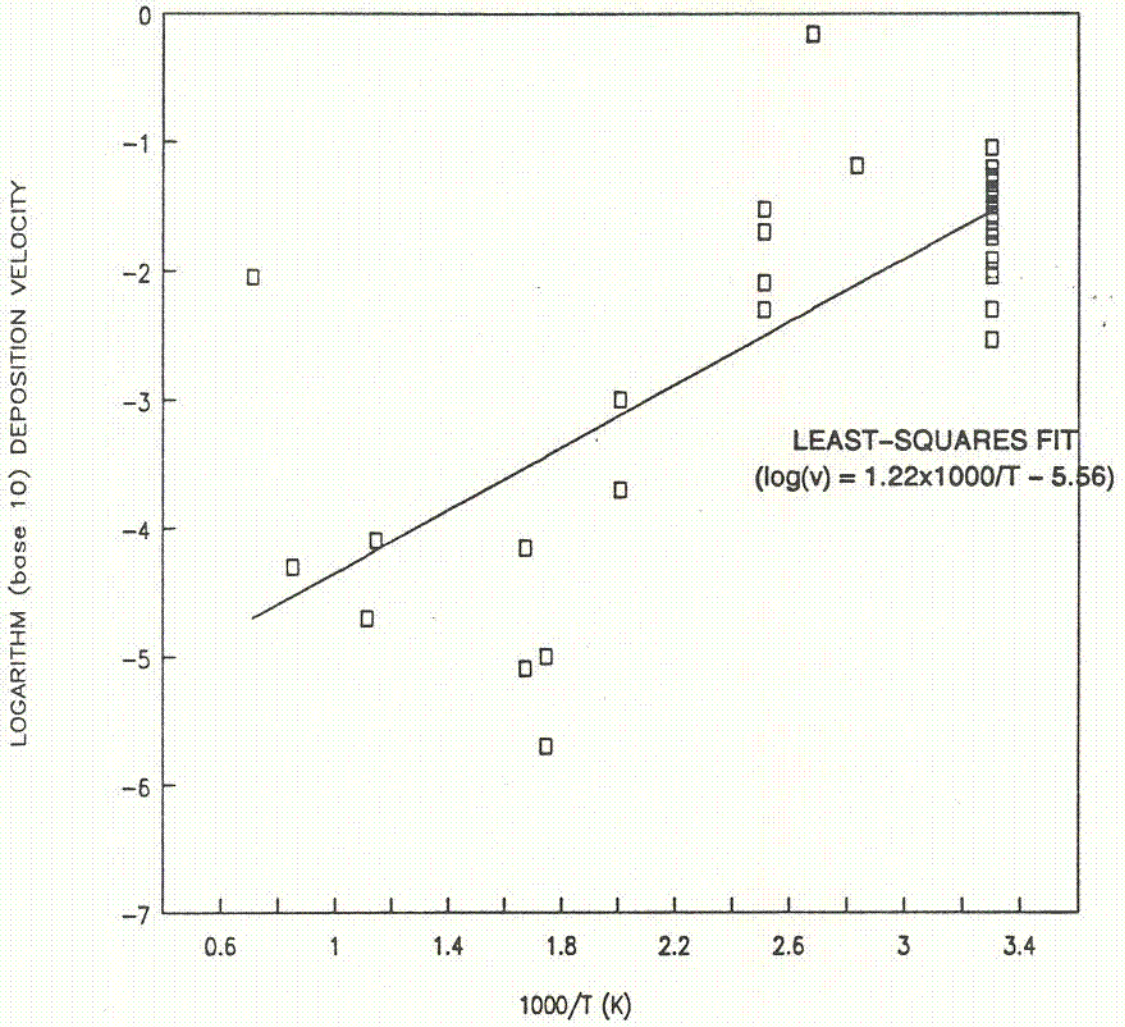## ELEMENTAL IODINE ON STAINLESS STEEL 304

Figure 2. Deposition Velocity Data and the Least-Squares Fit to the Data.

Deposition Velocities

The equation for deposition velocity of elemental iodine is based on the least–squares fit to the data in Table 1. Deposition equations for HOI and organic iodine are based upon the values at 30°C shown in Table 2 and an assumption that their temperature relationships have parallel curves to that for elemental iodine. Deposition of these latter two species is a relatively small effect and the accuracies of these two coefficients is not usually important to the transport analyses.

A. Elemental Iodine: $\quad d_{SI} = e^{(2809/T - 12.80(\pm 0.33))}$,

B. HOI: $\quad d_{SH} = e^{(2809/T - 15.39)}$, and

C. Organic Iodine: $\quad d_{SO} = e^{(2809/T - 19.30)}$.

Figure 3 shows a graph these three functions of deposition velocity and temperature.

Resuspension Rates

Resuspension rate equations as a function of temperature are based on the average rates at ambient temperature given in Table 1 and on an assumed temperature relationship (assumed because of a lack of data). The assumptions are that the resuspension rate will increase with increased temperature and that the equation take the form for the conventional chemical reaction rates (Arrhenius equation). The temperature coefficient in the equation is "an educated estimate" that forces the average value from the measurements at 30°C.

A. Elemental Iodine: $\quad v_I = 2.32(\pm 2.00) \times 10^{-5} e^{-600/T}$,

B. HOI: $\quad v_H = 5.65(\pm 2.20) \times 10^{-7} e^{-600/T}$, and

C. Organic Iodine: $\quad v_O = 6.81(\pm 3.20) \times 10^{-7} e^{-600/T}$.

Figure 4 shows graphs of the resuspension–temperature relations.

Surface Fixation Rate

The surface fixation rate equation is based upon the assumptions similar to those for the resuspension rates. The temperature coefficient here also is a best estimate that forces the average experimental value at ambient temperature from Table 1.

$$\phi = 1.30(\pm 0.75) \times 10^{-4} e^{-1185/T}.$$

Figure 5 shows the fixation rate as a function of temperature.
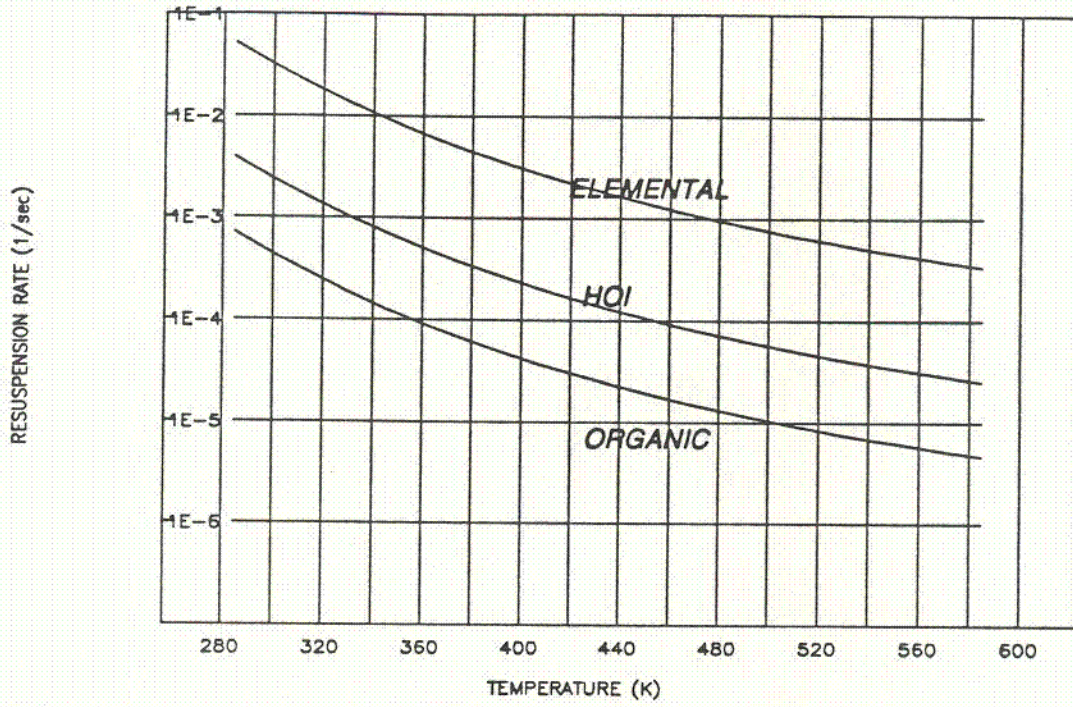
12

RESUSPENSION RATE

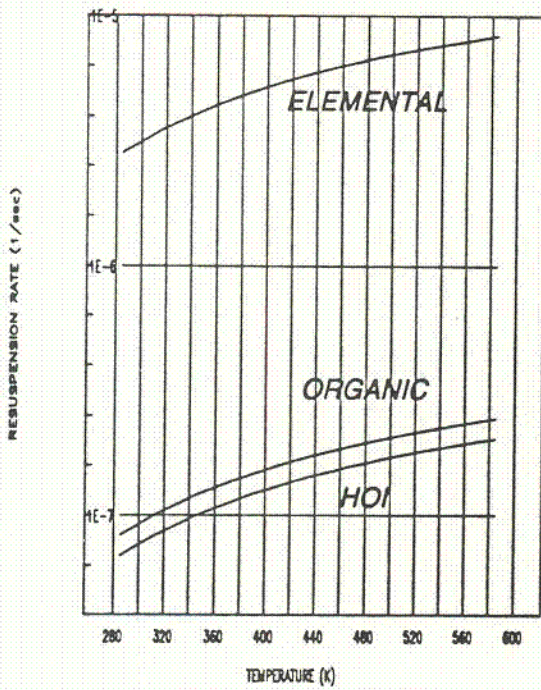FIGURE 3. Deposition Velocities as a Function of Temperature.

RESUSPENSION RATE

FIGURE 4. Resuspension Rates as a
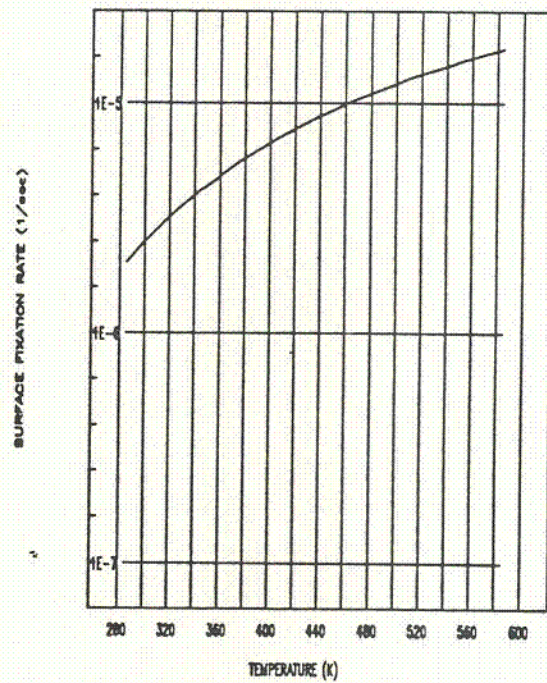Function of Temperature.

SURFACE FIXATION RATE

FIGURE 5. Surface Fixation Rate as a
Function of Temperature.

13

3.0   APPLICATION TO MSIV LEAKAGE

3.1   IODINE TRANSPORT RELATED TO MSIV LEAKAGE

Leakage of the main–steam–isolation valves (MSIV) following a loss–of–coolant accident (LOCA) could result in gaseous iodine transported from containment through steam piping into the condenser and subsequently into the turbine building atmosphere. The projected primary path is through the MSIVs, main steam lines and drain lines to the main condensers and out through the low–pressure turbines. These paths provide a low-velocity flow through relatively long and large diameter piping to a condenser also having a large volume. In this progression through the piping, iodine is continually interacting with the pipe interior surfaces, depositing, converting, resuspending, and permanently fixing to the surface, while undergoing radioactive decay. The transport of gaseous radioiodine from the containment atmosphere to the release point from the plant results in the complete deposition of gaseous elemental iodine and partial conversion to the other gaseous forms. The effective transport time of the iodine lengthens and the airborne release from the system has a time distribution that shows an equilibrium build up of the iodine resulting from surface activity build up and subsequent resuspension. A consequence of this amended time distribution of the release is in the dose assessments for different periods following a LOCA.

The containment atmosphere source term assumed for application of iodine transport models is U.S.N.R.C Regulatory Guide 1.3 which predicted that 25% of the core inventory of iodine will be airborne with a distribution of 96% elemental (elemental plus particulate) and 4% organic. Assumptions for purposes of analysis are: 1) that the containment leaks at a constant flow rate through each of the four MSIV and at a rate low enough that it does not deplete the containment concentration, 2) that the flow moves as a partial plug flow through the piping and as dilution within the large condenser. The model does not consider the scrubbing effects of liquids in the piping and condenser from steam condensing on the surface although, if present, liquids would reduce the resuspension of deposited iodine.

Figure 6 shows a sketch of the pathway assumed for purposes of computation. Table 3 shows the pipe segment lengths, diameters, MSIV leakage rates and other parameters assumed for the test case computations. The computations also assume an initial temperature and a cooling rate for each of the pipe segments. These data are based on assumptions of insulating lagging, heat transfer rates and a pipe mass for each leg and allowed temperature computations as a function of time after shutdown for each segment. Table 3 includes these the data for these assumptions. Figure 7 shows the results of the temperature computations for the main steam lines, drain lines and drain–line header as a function of time. Table 3 also includes the assumed values for primary iodine source term and containment and condenser volumes for the computations.
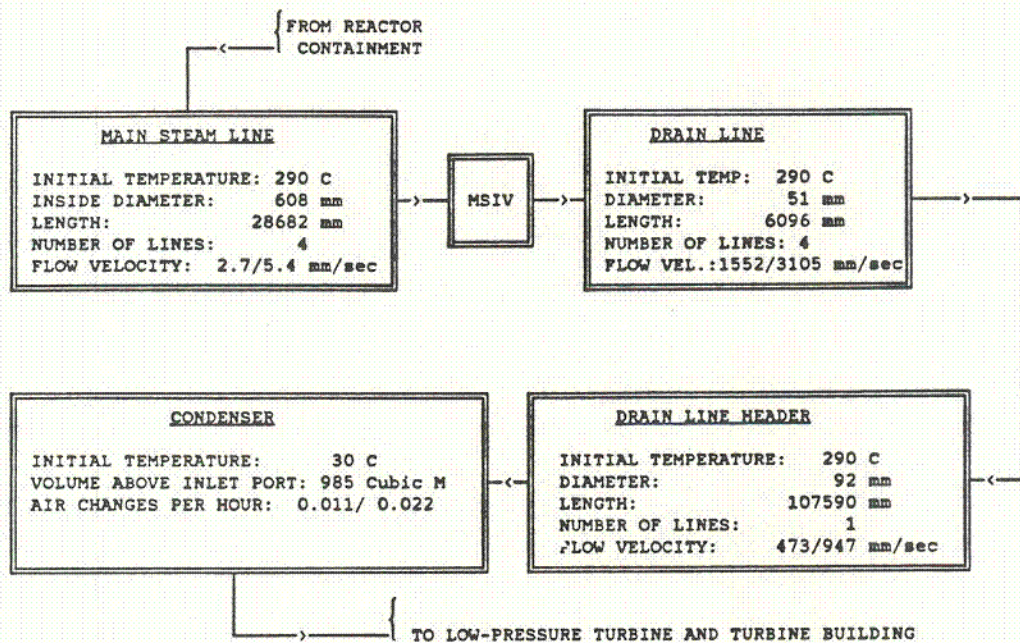
14

FIGURE 6. Schematic of MSIV Leakage Pathway from Containment to Release into the Turbine Building.

TABLE 3. Parameters Assumed for MSIV Leakage Analysis.

COMPONENT	PIPE DIAMETER	PIPE LENGTH	PIPE THICKNESS	PIPE MASS PER LENGTH	INSULATION THICKNESS
MAIN STEAM	60.8 cm	2868 cm	2.5 cm	490 kg/M	10.2 cm
DRAIN LINE	5.1 cm	610 cm	1.1 cm	8.7 kg/M	2.5 cm
DRAIN HEADER	9.2 cm	10759 cm	1.1 cm	28.3 kg/M	2.5 cm
CONDENSER	Volume: 985 M³		none		

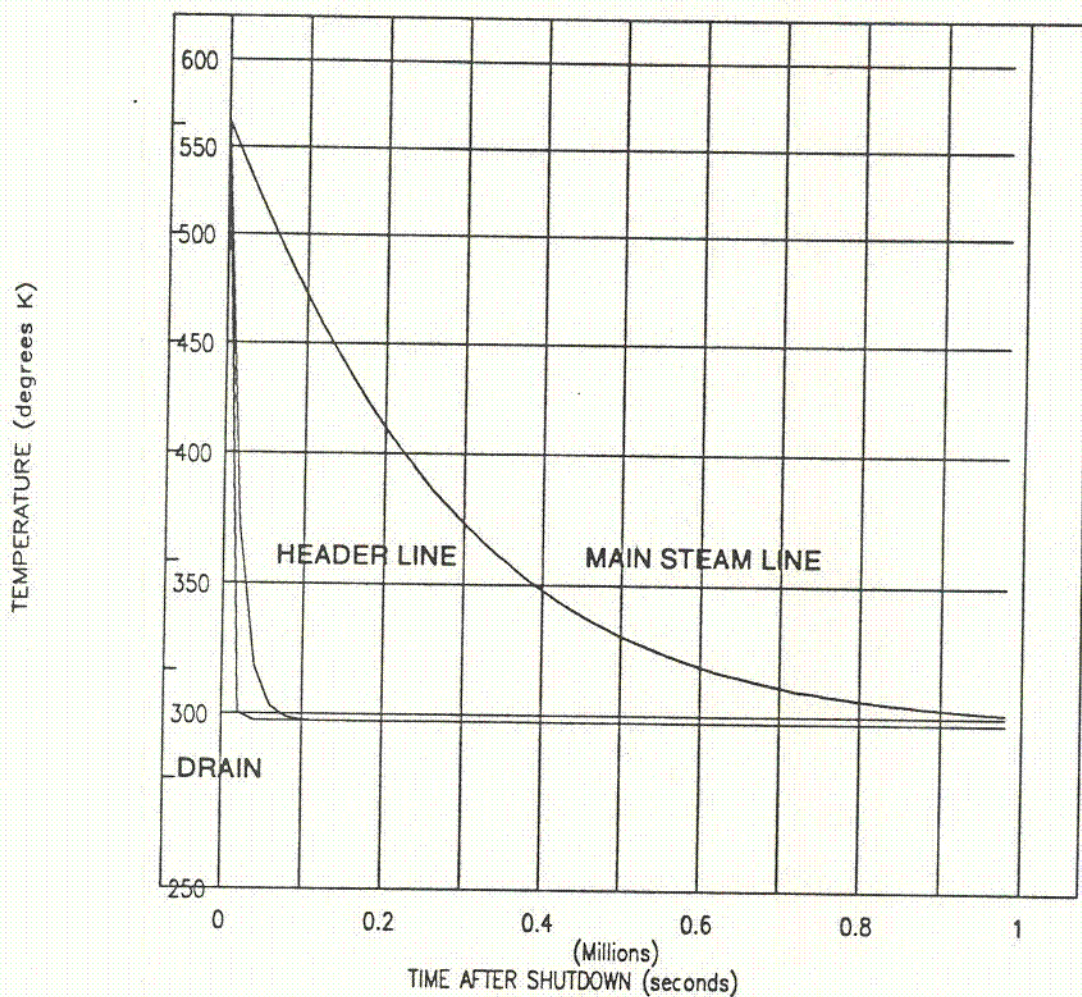LEAKAGE PER VALVE: 2.83 M³ AND 5.66 M³

15

FIGURE 7. Temperature of the MSIV Leakage Pathway Piping as a Function of Time after Shutdown. The Rate of Cooling is Nearly Independent of the Flow Rate at the Low Rates Considered in the Present Analysis.

16

3.   MODEL APPLICATIONS

Computations used the transport models described in Section 1, deposition, resuspension and fixation coef icient equations discussed in Section 2, and MSIV leakage parameters presented in Section 3.1 to estimate the ai borne iodine concentrations and integrated releases for MSIV leakage rates of 100 and 200 SCFH per valve. The computations required a total of 35,000 length segments in order to assure validity of the assumption of instantaneous mixing of the input concentration within the segment volume for calculation convergence.

3.2.1   IODINE CONCENTRATIONS

100–SCFH LEAKAGE per MSIV

CONDENSOR INLET CONCENTRATIONS

Figure 8 shows the input airborne iodine concentrations to the condenser for a 100 SCFH leakage per MSIV. The data include radioactive decay of the source as well as both decay and surface fixation during transit through the piping. The concentrations are in fractional units of the total airborne iodine concentration in   containment at time, t=0. Organic concentrations include the 4% initial organic component and the deposited iodine resuspended from the surfaces whereas the HOI component arises wholly from resuspended surface iodine. The concentration of elemental iodine shows the effect of cooling of the pipe during the 30–day release time. Initial deposition was relatively low because of the low deposition rate at higher temperatures.

CONDENSER OUTLET CONCENTRATIONS

Figure 9 shows the condenser outlet concentrations as a function of time for the 100–SCFH analysis. The concentration units are those used in Figure 2, relative to the total airborne iodine concentration in containment at time, t=0. The Figure shows four curves. The upper two curves show the airborne concentrations of organic and inorganic (HOI) iodine resulting from the same species injected into the condenser. The lower two curves are for organic and inorganic iodine resuspended from elemental iodine injected into the condenser and deposited on the surfaces. These contributions at 100 SCFH leakage rate are nearly negligible. The curves early in the release, when compared to the input data in Figure 8, show the effects of dilution of the low flow into the large condenser volume.

200–SCFH LEAKAGE per MSIV

CONDENSOR INLET CONCENTRATIONS

Figure 10 shows the input airborne iodine concentrations to the condenser for a 200 SCFH leakage per MSIV. These data also include radioactive decay of the source as

17

MSIV LEAKAGE RELEASES TO CONDENSER

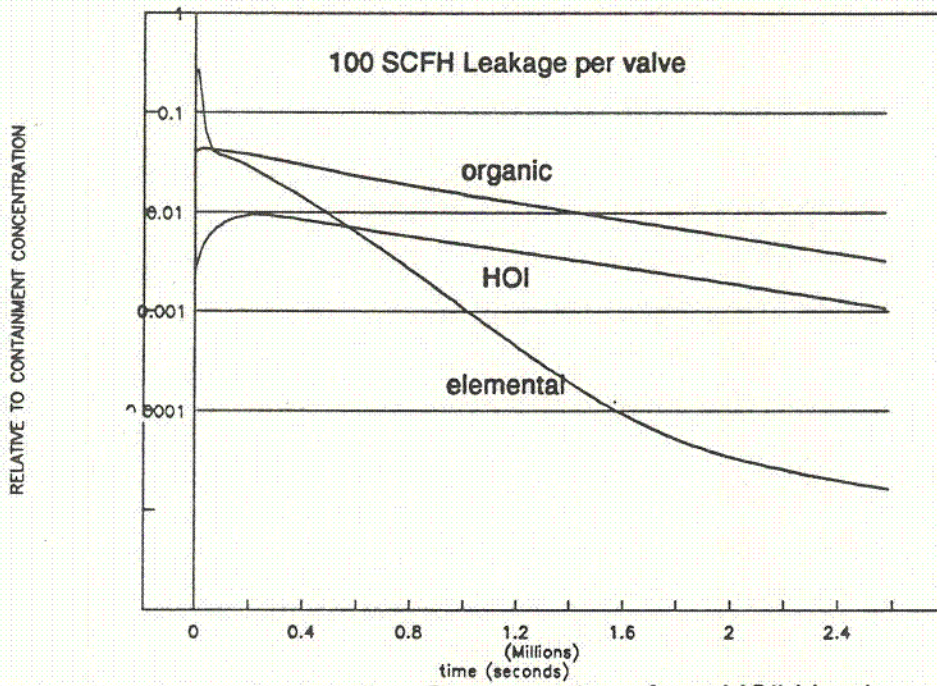## RELATIVE IODINE EFFLUENT CONCENTRATIONS

FIGURE 8. Condenser Inlet Iodine Concentrations from MSIV Leakage at 100 SCFH.

MSIV LEAKAGE RELEASES FROM CONDENSER

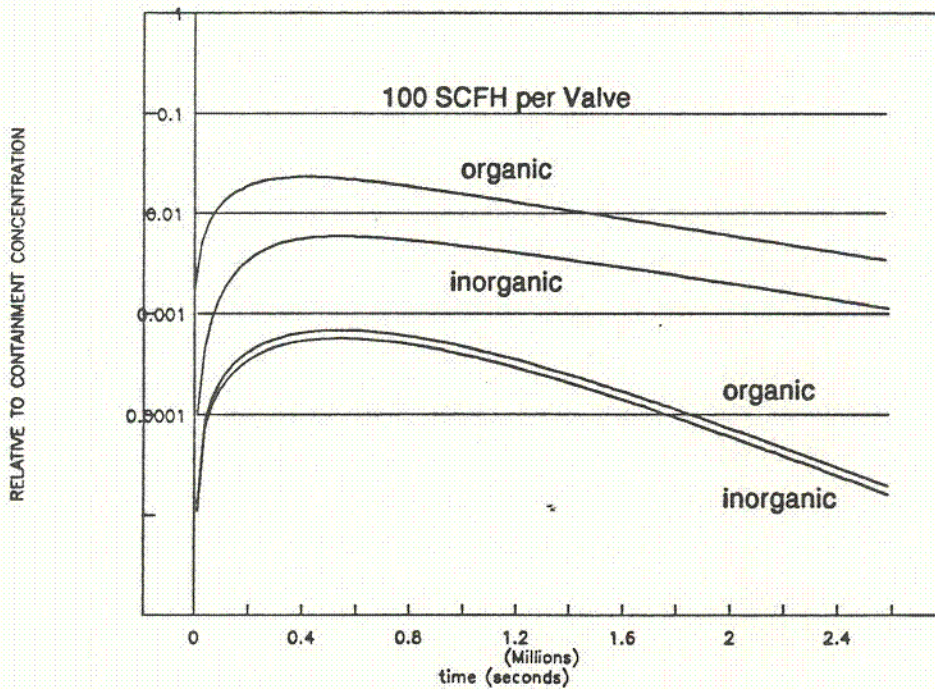## RELATIVE IODINE EFFLUENT CONCENTRATIONS

FIGURE 9. Condenser Outlet Iodine Concentrations for 100 SCFH MSIV Leakage.

18

well as both decay and surface fixation during transit through the piping. The concentrations here also are in fractional units of the total airborne iodine concentration in containment at time, t=0. Organic concentrations include the 4% initial organic component and the deposited iodine resuspended from the surfaces whereas the HOI component arises wholly from resuspended surface iodine. The concentration of elemental iodine, when compared to comparable data at 100 SCFH shows the increased transmission due to the shorter pipe residence time in the higher flow.

CONDENSER OUTLET CONCENTRATIONS

Figure 11 shows the condenser outlet concentrations as a function of time for the 200–SCFH analysis. The concentration units are the same as previously presented. As done with the data at 100 SCFH leakage, the Figure shows four curves representing airborne concentrations of organic and inorganic (HOI) iodine resulting from the same species injected into the condenser and that resuspended from elemental iodine injected into the condenser and deposited on the surfaces. These contributions at 200 SCFH leakage rate are significantly higher than those at 100 SCFH because of the higher transmission of elemental iodine into the condenser.

3.2.2 INTEGRATED IODINE RELEASES

100–SCFH LEAKAGE per MSIV

CONDENSER INTEGRATED INLET ACTIVITY

Figure 12 shows the integrated relative total activity, by species for leakage into the condenser at a rate of 100 SCFH per MSIV. The curves are cumulative with the area between the curves representing the total release of that species at the corresponding time.

CONDENSER OUTLET INTEGRATED RELEASES

Figure 13 presents the integrated release from the condenser, units of total Curies of ^{131}I, by species. The data are cumulative, showing the contributions from condenser inlet inorganic (HOI) and that resuspended, and organic, inlet and resuspended as areas between the curves.

200–SCFH LEAKAGE per MSIV

CONDENSER INTEGRATED INLET ACTIVITY

Figure 14 shows the relative integrated total input to the condenser at a leakage rate of

19

MSIV LEAKAGE RELEASES TO CONDENSER
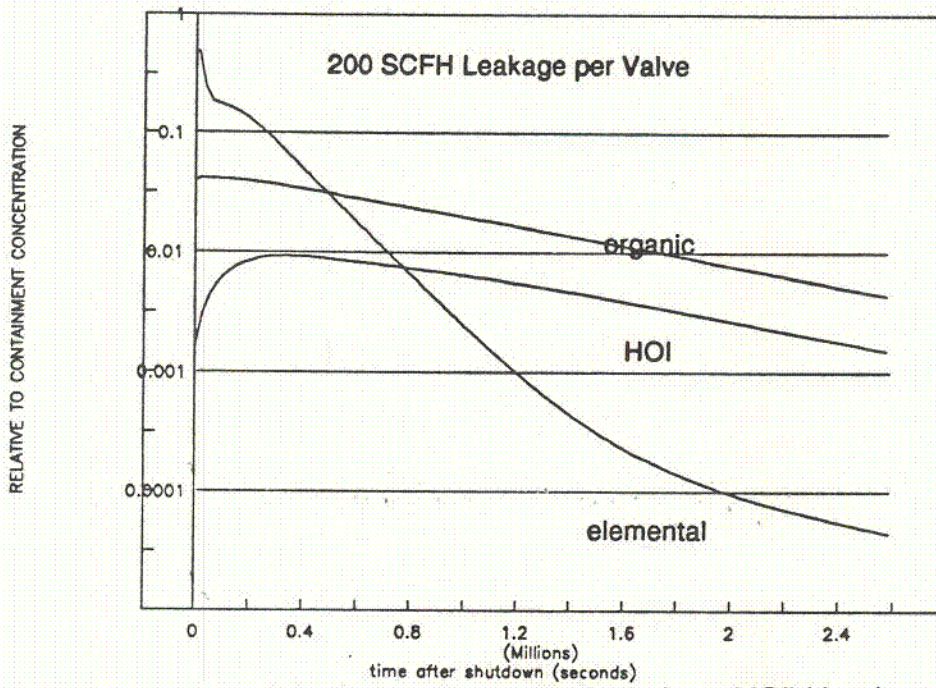### RELATIVE IODINE EFFLUENT CONCENTRATIONS

FIGURE 10. Condenser Inlet Iodine Concentrations from MSIV Leakage at 200 SCFH.

MSIV RELEASES FROM CONDENSER
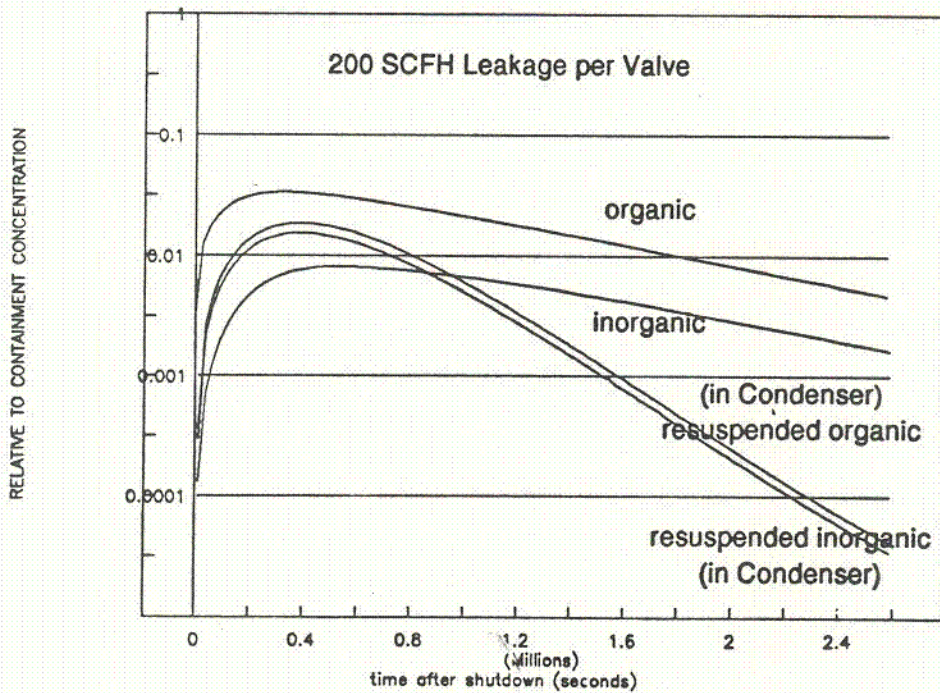### RELATIVE IODINE EFFLUENT CONCENTRATIONS

FIGURE 11. Condenser Outlet Iodine Concentrations for 200 SCFH MSIV Leakage.
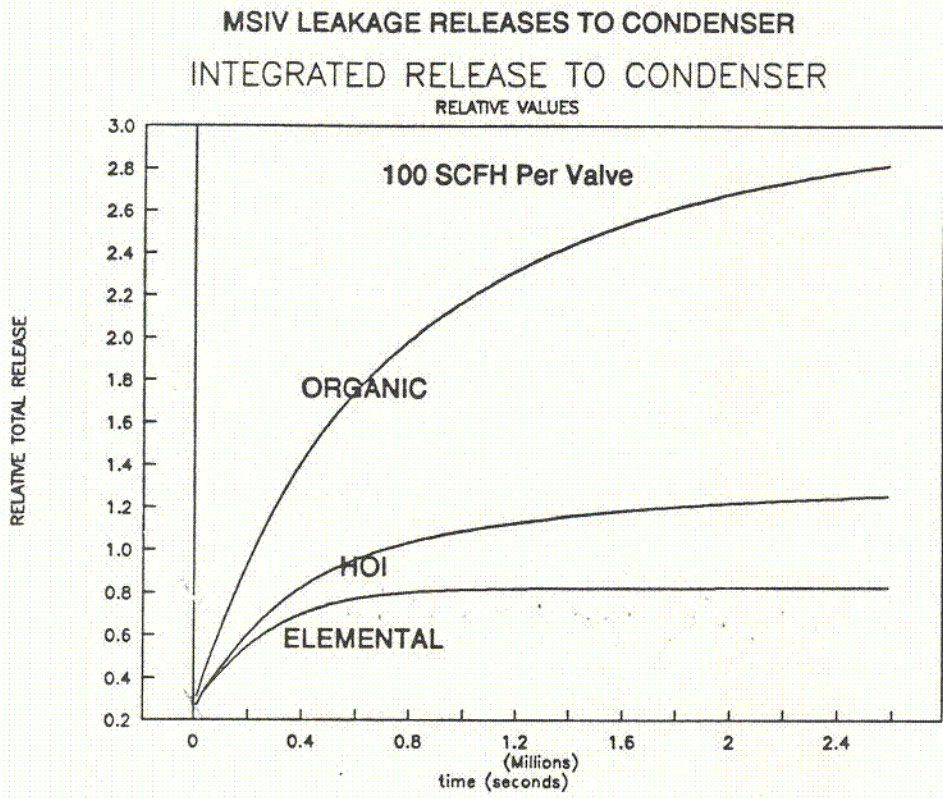
20

MSIV LEAKAGE RELEASES TO CONDENSER

INTEGRATED RELEASE TO CONDENSER
RELATIVE VALUES

FIGURE 12. Integrated Condenser Inlet Total Iodine for MSIV Leakage at 100 SCFH.

MSIV LEAKAGE RELEASES FROM CONDENSER
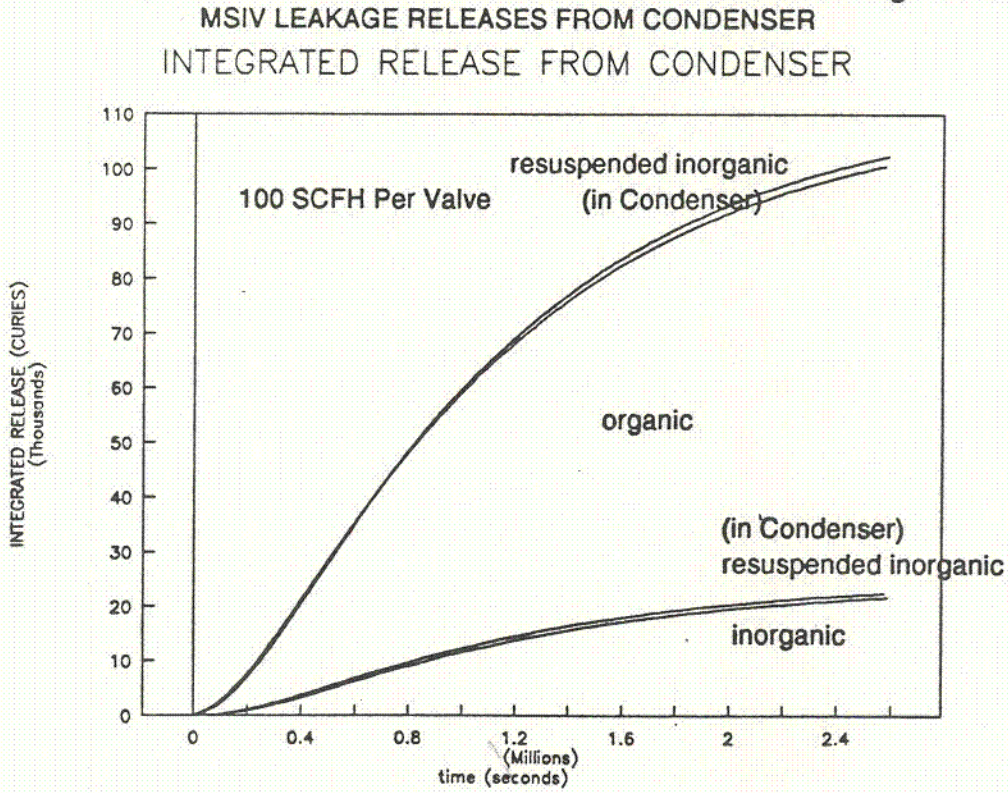
INTEGRATED RELEASE FROM CONDENSER

FIGURE 13. Integrated Condenser Outlet Total Iodine for MSIV Leakage at 100 SCFH.

21

200 SCFM per MSIV. The curves are cumulative with the area between the curves representing the total release of that species at that time.

CONDENSER OUTLET INTEGRATED RELEASES

Figure 15 presents the integrated release from the condenser at a leakage rate of 200 SCFH, units of total Curies of ^{131}I, by species. The data are cumulative, showing the contributions from condenser inlet inorganic (HOI) and that resuspended, and organic, inlet and resuspended as areas between the curves.

3.3 SUMMARY OF TRANSPORT ANALYSES

Table 4 summarizes the parameters for the analyses of the iodine transport for an MSIV leakage of 100 SCFH per valve. Data in the Table include the condenser and containment volumes and the core inventory of ^{131}I at the time of shutdown. Deposition velocities, and resuspension and surface fixation rates in the Table are those at 30°C. The Table also lists the total iodine release from the condenser, including both organic and inorganic (HOI) species, at times of 2, 4, 24, 96, and 720 (30 days) hours. Included is the integrated activity into the condenser. The differences are from decay during the dilution delay.

Table 5 presents similar data for a leakage rate of 200 SCFM per MSIV. Here the proportional losses within the condenser are less because of the higher flow rate and consequent shorter holdup from dilution.
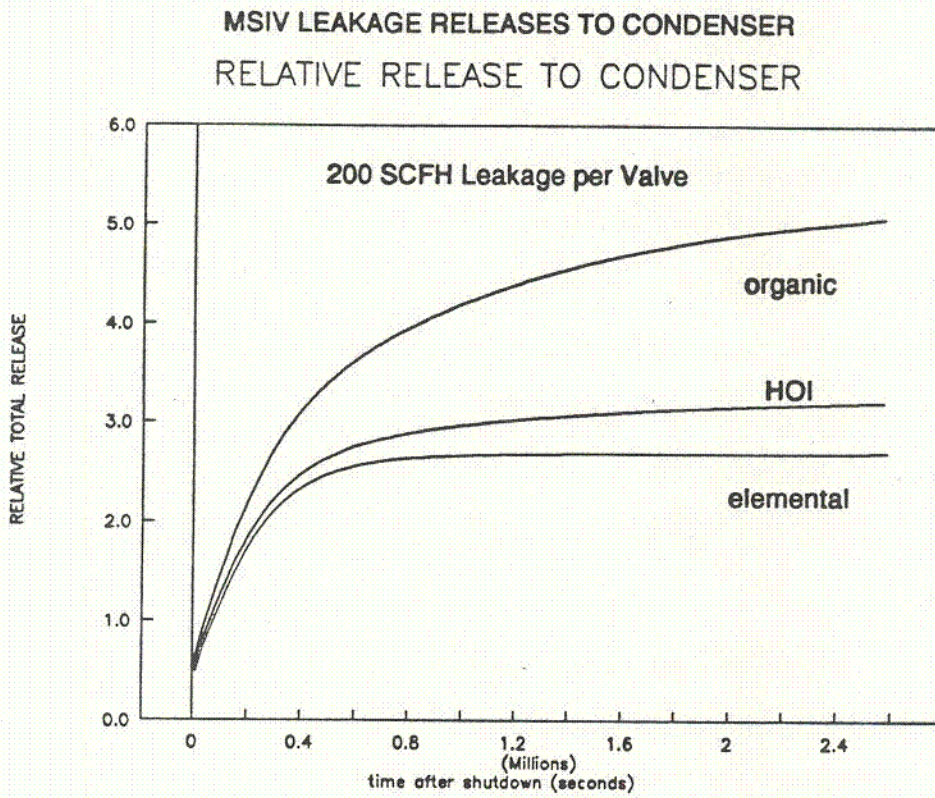
RELATIVE RELEASE TO CONDENSER

FIGURE 14. Integrated Condenser Inlet Total Iodine for MSIV Leakage at 200 SCFH.

MSIV LEAKAGE RELEASES FROM CONDENSER

INTEGRATED RELEASE FROM CONDENSER

FIGURE 15. Integrated Condenser Outlet Total Iodine for MSIV Leakage at 200 SCFH.

MSIV LEAKAGE ANALYSIS FOR HOPE CREEK

INPUT PARAMETERS:

INLET CONCENTRATION:	1
(FRACTION OF INITIAL CONTAINMENT CONCENTRATION)	
TOTAL INLET LEAK FLOW RATE(cm/sec):	3115
ELEMENTAL FRACTION:	0.96
DEPOSITION VELOCITY(cm/sec):	3.22E-02
RESUSPENSION RATE(1/sec):	3.14E-06
HOI FRACTION:	0
DEPOSITION VELOCITY(cm/sec):	1.77E-04
RESUSPENSION RATE(1/sec):	7.65E-08
ORGANIC FRACTION:	0.04
DEPOSITION VELOCITY(cm/sec):	4.84E-05
RESUSPENSION RATE(1/sec):	9.22E-08
SURFACE FIXATION RATE(1/sec):	2.50E-06
INJECTION TIME(sec):	2600000
PIPE DIAMETERS(cm):	60.8,5,9.2
PIPE LENGTHS(cm):	2868,610,10754
CONDENSER VOLUME(cc):	9.85E+08
CONTAINMENT VOLUME(cc):	2.72E+10
REACTOR CORE IODINE INVENTORY (CURIES):	8.7E+07

TOTAL RELEASES (CURIES)

TIME PERIOD	INLET	INLET	CONDENSER OUTLET
2 hr:	3.8E+04	1.2E+04	6.9E+01
4 hr:	1.0E+05	2.5E+04	3.4E+02
24 hr:	2.4E+05	3.8E+04	1.7E+03
96 hr:	7.5E+05	8.4E+04	1.7E+04
720 hr:	2.3E+06	2.1E+05	1.0E+05

MSIV LEAKAGE ANALYSIS FOR HOPE CREEK	
INPUT PARAMETERS:	
INLET CONCENTRATION:	1
(FRACTION OF INITIAL CONTAINMENT CONCENTRATION)	
TOTAL INLET LEAK FLOW RATE(cm/sec):	6292.8
ELEMENTAL FRACTION:	0
DEPOSITION VELOCITY(cm/sec):	1.28E+01
RESUSPENSION RATE(1/sec):	2.32E-05
HOI FRACTION:	0
DEPOSITION VELOCITY(cm/sec):	1.80E+01
RESUSPENSION RATE(1/sec):	5.65E-07
ORGANIC FRACTION:	0
DEPOSITION VELOCITY(cm/sec):	1.93E+01
RESUSPENSION RATE(1/sec):	6.81E-07
SURFACE FIXATION RATE(1/sec):	2.49E-06
INJECTION TIME(sec):	2600000
PIPE DIAMETERS(cm):	9.20
PIPE LENGTHS(cm):	1000.00
CONDENSER VOLUME(cc):	9.8E+08
CONTAINMENT VOLUME(cc):	2.72E+10
REACTOR CORE IODINE INVENTORY (CURIES):	8.7E+07

TOTAL RELEASES (CURIES)

TIME PERIOD	INLET	INLET	CONDENSER OUTLET		
2 hr:	7.7E+04	4.2E+04	3.2E+02	1.83	131
4 hr:	2.1E+05	9.2E+04	2.0E+03		
24 hr:	4.8E+05	1.6E+05	1.0E+04		
96 hr:	1.5E+06	3.7E+05	9.1E+04		
720 hr:	4.7E+06	7.4E+05	4.2E+05	..3:	1.76

Total F

11.2

REFERENCES

1.   Vapor Deposition Velocity Measurements and Consolidation for I_2 and CsI, *NUREG/CR-2713*, S.L.Nicolosi and P.Baybutt, May 1982.

2.   Fission Produce Deposition and Its Enhancement Under Reactor Accident Condition: Deposition on Primary–System Surfaces, *BMI–1863*, J.M.Genko *et.al.*, May 1969.

3.   Transmission of Iodine Through Sampling Lines, *18th DOE Nuclear Airborne Waste Management and Air Cleaning Conference*, P.J.Unrein, C.A.Pelletier, J.E.Cline and P.G.Voillequè, October 1984.

4.   Deposition of ^{131}I in CDE Experiments, *IN-1394*, Nebeker *et.al.*, 1969.

5.   In–Plant Source Term Measurements at Prairie Island Nuclear Generating Station, *NUREG/CR-4397*, J.W.Mandler, A.C.Salker, S.T.Croney, D.W.Akers, N.K.Bihl, L.S.Loret and T.E.Young, September 1985.

6.   Measurements of [129]I and Radioactive Particulate Concentrations in the TMI-2 Containment Atmosphere During and After the Venting, SAIC-139-80-573-LJ/GEND-009, *J.E.Cline et.al., October 1980*.

7.   *Station Blackout at Brown's Ferry Unit One--Iodine and Nobel Gas Distribution and Release, NUREG/CR-2182, Volume 2,* R.P.Wichner, W.Davis, Jr., C.F.Weber, R.A.Lorenz, and A.D.Michell, August 1978.

8.   Series of Measurements and Reports by SAIC to Individual Utilities, (BWR A) October 1988, (PWR A) December 1988, (BWR B) *SAIC–89/1N422* June 1990, (PWR B) July 1989, (BWR C) September 1989, (PWR C) *SAIC–89/1756* December 1989, (PWR D) *SAIC–90/1355* August 1990, (BWR D) October 1990.

9.   Deposition of Airborne Radioiodine Species on Surfaces of Metals and Plastics, *17th DOE Nuclear Air Cleaning Conference*, M.J.Kabat, October 1982.

10. Results of Independent Measurements of Radioactivity in Process Streams and Effluents at Boiling Water Reactors, *USAEC Report*, compiled by C.A.Pelletier, May 1973.

11. Sources of Radioiodine at Boiling Water Reactors, *EPRI NP-495*, C.A.Pelletier, E.D.Barefoot, J.E.Cline, R.T.Hemphill, W.A.Emel, and P.G.Voillequè, February 1978.

12. Sources of Radioiodine at PWRs, *EPRI NP-939*, C.A.Pelletier, E.D.Barefoot, J.E.Cline, R.T.Hemphill, W.A.Emel, and P.G.Voillequè, November 1978.

13. Line–Loss Determination for Air Sampler Systems, *NUREG/CR-4757 PNL-7597*, J.A.Glissmeyer & G.A.Sehmel, February 1991.